Journal of
Nanoscience and Nanotechnology
Vol. 9, 6228–6233, 2009

Purification and Functionalization of Carbon Nanotubes by Classical and Advanced Oxidation Processes

M. Escobar[1,2], S. Goyanes[2], M. A. Corcuera[3,*], A. Eceiza[3], I. Mondragon[3], G. H. Rubiolo[2,4], and R. J. Candal[1]

[1] *Instituto de Fisicoquímica de Materiales, Ambiente y Energía, CONICET-UBA. Ciudad Universitaria 1428 Bs As, Argentina*
[2] *LP&MC, Dep. de Física, FCEyN-UBA, Pab1, Ciudad Universitaria 1428 Bs As, Argentina*
[3] *'Materials + Technologies' Group, Dpto. Ingeniería Química y M. Ambiente. Escuela Politécnica. Universidad País Vasco/ Euskal Herriko Unibertsitatea. Pza. Europa 1. 20018 Donostia-San Sebastián, Spain*
[4] *Unidad de Actividad Materiales, CNEA, Av Gral. Paz 1499, San Martin (1650), Bs As, Argentina*

Advanced oxidation technologies (AOT) were applied for the production of accurately controlled oxidized multi-walled carbon nanotubes. Fenton process is effective to get carboxylic ($-COO^-$ or $-COOH$) and OH groups on the surface of carbon nanotubes while Photofenton and UV/H_2O_2 processes mostly produce OH groups on surface of multiwalled carbon nanotubes (MWCNT). All of them preserve the structure of MWCNT allowing to achieve accurately controlled oxidized MWCNT. Fourier transform infrared spectroscopy (FTIR) and thermogravimetical analysis (TGA) show that the acid treatment is the more efficient technique to generate COOH groups on MWCNT surface. However, this chemical technique generates strong damages on the MWCNT structure, as demonstrated by TGA, field emission scanning electron microscopy and transmission electron microscopy results.

Keywords: Carbon Nanotubes, Fenton, Photo-Fenton, Controlled Oxidation.

1. INTRODUCTION

Multiwalled carbon nanotubes (MWCNT) are usually produced by arc discharge, laser ablation and chemical vapor deposition (CVD). In all cases, the as-grown carbon nanotubes (CNT) contain different and important amounts of impurities, such as amorphous carbon, silicon dioxide (or iron silicates) and metallic particles. Since all these impurities cause a serious impediment for detailed characterizations and advanced applications, they need to be removed by physical or chemical processes. On the other hand, the functionalization of CNT is necessary to improve the compatibility between CNT and matrix for their applications as reinforcement in polymers.[1–3]

One of the first steps in CNT functionalization is the introduction of OH or carboxylic groups on the surface of the tubes, which is usually performed by slight oxidation of the carbonaceous structure. Oxidative acid attack is one of the most used techniques for both purification and oxidation of CNT.[4–7] The acid treatment typically involves the use of concentrated sulfuric and nitric acid. Due to the combination of strong acidic and oxidative capacity, this mixture is ideal to dissolve SiO_2, metallic particles and to eliminate amorphous carbon. Unfortunately, the reaction goes easily out of control and the CNT result damaged during the treatment. Besides, the combination of two concentrated acids is not easy to handle and may be dangerous for workers and the environment. The problem is even worst in the case of massive scale production (as may be necessary for the production of CNT for polymer reinforcement).

The newly developed advanced oxidation technologies (AOT) are interesting alternatives for the production of accurately controlled oxidized CNT, avoiding the use of concentrated acids, and keeping most of their properties intact. AOT involve the generation and use of transient species with great oxidation power, like the radical $OH^{\cdot}$. Besides, these technologies are simple and friendly with the environment and also not dangerous for the operator during its industrial application.

Recently, AOT have been applied for CNT surface oxidation as, i.e., UV/Ozone[8] and hydrogen plasma[9] treatments. Ying et al. were the first to introduce new routes to covalently functionalize nanotubes by addition of free

*Author to whom correspondence should be addressed.

1533-4880/2009/9/6228/006 doi:10.1166/jnn.2009.1563

radicals.[10] Li et al.[11] reported the oxidation of MWCNT using Fenton's reagent, namely ferrous salt and hydrogen peroxide mixture (Fe^{2+}–H_2O_2), showing that MWCNT can be oxidized successfully by the hydroxyl radical $OH^{\cdot}$.

The Fenton process involve the reaction between H_2O_2 and Fe(II):

$$Fe^{2+} + H_2O_2 \rightarrow Fe^{3+} + HO^- + OH^{\cdot} \quad (1)$$

$$Fe(II) + OH^{\cdot} \rightarrow Fe(III) + HO^- \quad (2)$$

At pH lower than 3, the reaction is autocatalytic[12, 13] because the Fe(III) decompose H_2O_2 in H_2O and O_2 through a mechanism in chain:

$$Fe^{3+} + H_2O_2 \rightarrow Fe\text{-}OOH^{2+} + H^+ \quad (3)$$

$$Fe\text{-}OOH^{2+} \rightarrow HO_2^{\cdot} + Fe^{2+} \quad (4)$$

$$Fe^{2+} + H_2O_2 \rightarrow Fe^{3+} + HO^- + HO^{\cdot} \quad (5)$$

$$HO_2^{\cdot} + Fe^{2+} + H^+ \rightarrow Fe^{3+} + H_2O_2 \quad (6)$$

$$HO_2^{\cdot} + Fe^{3+} \rightarrow Fe^{2+} + O_2 + H^+ \quad (7)$$

$$OH^{\cdot} + H_2O_2 \rightarrow H_2O + HO_2^{\cdot} \quad (8)$$

The parameters that should be controlled to reach optimum activity are the ratio Fe^{2+}/H_2O_2, the relative amount of the material to be oxidized and the temperature.

There is an extension of Fenton process, called Photo-Fenton, which takes advantage of UV light irradiation at wavelength lower than 360 nm. The irradiation of Fe(III) hydroxo-complexes by light produces their photolysis and the generation of $OH^{\cdot}$ radicals:

$$Fe(III)(OH)^{2+} + h\nu \rightarrow Fe(II) + OH^{\cdot} \quad (9)$$

The photogenerated Fe(II) produces additional HO that generates more OH through reaction (1). The amount of Fe(II) needed to keep the process working is considerably lower than in Fenton process.[14]

Another potential AOT for the oxidation of MWCNT could be the UV/H_2O_2 process based in the cleavage of the H_2O_2 molecule under irradiation of light with wavelength of 220 nm:

$$H_2O_2 \rightarrow 2HO^{\cdot} \quad (10)$$

To the best of our knowledge, there has been no one work reporting modification of MWCNT by Photo-Fenton and UV/H_2O_2 processes. However, Rao[15] reported UV-light accelerated oxygen adsorption to carbon nanotubes and changes in their thermoelectric power. In the present study, we employed Fenton, Photo-Fenton and UV/H_2O_2 processes to oxidize MWCNT and systematically investigated the effect of hydroxyl radical ($HO^{\cdot}$) on the structure of MWCNT with the aid of Fourier transform infrared spectroscopy (FTIR), thermogravimetrical analysis (TGA), field emission scanning electron microscopy (FE-SEM) and transmission electron microscopy (TEM) in an attempt to preserve their structure and properties. Results have been compared with those obtained by the traditional oxidative acid attack.

2. EXPERIMENTAL DETAILS

Carbon nanotubes were synthesized by the catalytic decomposition of acetylene over iron nanoparticles included in silicon matrix prepared by sol–gel method, as reported elsewhere.[16] The growth of MWCNT was performed at an absolute pressure of 180 torr.

The purification method consisted of removing of the silica support as follows. About 100 mg of MWCNT/silica were treated with 6 mL of a mixture of fluorhidric acid/sulfuric acid, 1:1 v/v. Then, they were rinsed twice with 10 mL of HCl (c) to dissolve all the iron present. After that, the suspension was centrifuged with distilled water until pH 6.

Different strategies based on the generation of the radical $OH^{\cdot}$ and also oxidative acid treatment were used to modify MWCNT. For each treatment 30 mg purified MWCNT were used. The first treatment was Fenton process: MWCNT were dispersed in 20 mL of distilled water using ultrasonic bath. Next, a 1.0 mL H_2O_2 (30%—Fluka) and 1.0 mL $FeSO_4$ (6×10^{-2} M) solutions were added in stepwise fashion with 30 min intervals under permanent stirring. The pH of the suspension during reaction was adjusted to 3 using H_2SO_4. In order to stop the reaction, ammonium was used to increase pH value. After that, the MWCNTs were washed with diluted hydrochloric acid to dissolve the remaining iron hydroxide, rinsed with water and centrifugated to separate the material from the solution. The cleaned MWCNT were dried at 80 °C in oven and stored. The carbon nanotubes treated with this method are named f-MWCNT.

The second treatment was Photo-Fenton process: the procedure was similar to the previous one but the reaction was carried out under UV radiation (150 W Hg lamp) using a quartz glass vessel. In this case, carbon nanotubes are called pf-MWCNT.

The third strategy was to disperse MWCNT in 20 mL H_2O_2 (30%) under UV light source (150 W Hg lamp) and continuous stirring. These carbon nanotubes are named u-MWCNT.

For comparison, a sample of CNT was oxidized by the classical method, using a 1:3, v/v mixture of nitric acid/sulfuric acid (see Ref. [5] for more details). In this case, sample is called a-MWCNT.

Scanning electron microscopy was conducted at 5 kV using a Zeiss LEO 982 GEMINI field emission scanning microscope. Transmission electron microscopy images were obtained in a Philips EM 301. Thermogravimetric analysis (Shimadzu TGA-51) was performed on 10 mg samples in air atmosphere using the following protocol: from room temperature to 120 °C at 10 °C/min, keeping this temperature for 20 min, and then 120–900 °C heating at 3 °C/min. FTIR spectra were collected using a Nicolet Magna 550. The KBr blank and the MWCNT samples were dried in vacuum oven at 130 °C for three hours prior

to take the spectra in order to eliminate all rest of water sorbed in the sample.

3. RESULTS AND DISCUSSION

As is well known, the CVD process produces CNT mixed with the silicate matrix that contains the catalytic iron nanoparticles. Figure 1(a) shows FE-SEM micrographs of the MWCNT without any cleaning treatment. A big particle of SiO_2 can be clearly seen. Figure 1(b) shows FE-SEM images of MWCNT after being purified by treatment with a mixture of hydrofluoric + sulfuric acid ($HF + H_2SO_4$) and washed with concentrated hydrochloric acid, HCl. Most of the silicate was removed by the combination of the acids and only small inclusions remained attached to some CNT. The cleaning procedure works as follows. The mixture of $H_2SO_4 + HF$ reacts with the silicates producing mostly $SiF_4(g)$, which is removed from the system, and soluble hexafluor-silicic acid, which remains in the system. To eliminate the remaining silicon, the system is washed with concentrated HCl acid. On this way the precipitation of silicic acid can be prevented. Finally the CNT are rinsed with water, ethanol and dried at 70 °C.

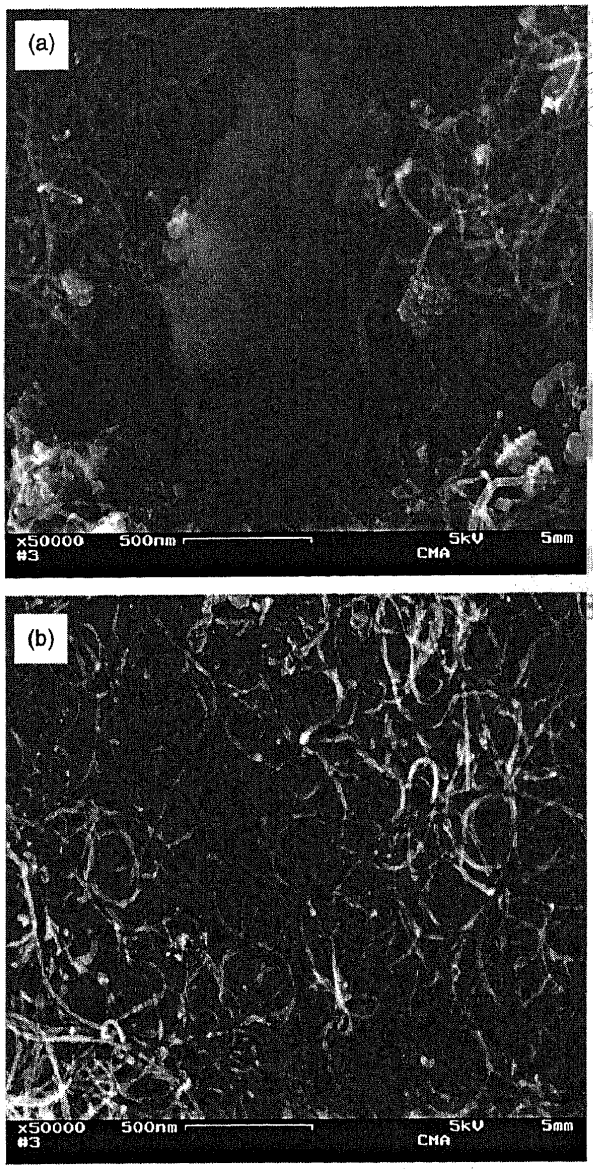

Fig. 1. (a) MWCNT-silica matrix obtained after carbon deposition, (b) purified MWCNT.

The cleaned MWCNT (Fig. 1(b)) were oxidized by application of the three different AOT and the oxidative acid attack. Figures 2(a–d) shows FTIR spectra of the samples before and after several treatment times. The cleaned CNT (named as "0 h" in all the figures) display features at 1080 and 1560 cm^{-1}, which correspond to Si–O stretching and CNT skeleton, respectively. Figure 2(a) shows the spectra of the MWCNT after different Fenton treatment times. Several new peaks can be identified in the spectra, which correspond to C=O stretching (1710 cm^{-1}), C–O stretching of COOH (1260 cm^{-1}), CH_x stretching (2853 and 2925 cm^{-1}), C=C ring stretching (1470 cm^{-1}) and O–H stretching (3450 cm^{-1}). The intensity of the features increases with the treatment time. It is worth to note that the new peak at 1470 cm^{-1} suggests that the Fenton treatment, besides of generating reactive groups, purifies the MWCNT. These results are in agreement to those reported by Li et al.[11] Figure 2(b) shows the effect of Photo-Fenton process on CNT. The spectra show similar features to those for the Fenton treatment. However, the intensity of the C=O stretching peak is lower while the intensity of OH stretching is higher. As can be seen from Figure 2(c), the UV/H_2O_2 treatment only introduces OH and CH_x groups in the CNT structure (features at 3450, 2925 and 2853 cm^{-1}, respectively). Moreover, the intensity of the features corresponding to OH and CH_x is notably higher than in the other AOT studied while the C=O stretching feature appears as a shoulder only after four hours of treatment.

The FTIR spectra of MWCNT treated with the oxidative acid attack are shown in Figure 2(d). This treatment introduces mainly C=O bonds on the CNT structure; the amount of OH and CH groups is notably lower in comparison with the AOT studied. The peak around 1080 cm^{-1}, corresponding to Si–O stretching, disappears showing an appreciable elimination of remaining silicon nanoparticles but, a new strong band appears at 1120 cm^{-1} due to sulphate groups generated by the process and sorbed on the walls of carbon nanotubes.

It should be noted that in all the treatments the intensity of C–H stretching mode increases with the reaction time, which may be related to the combination of hydrogen atoms with C terminal groups produced during MWCNT oxidation.

The different results obtained after the different treatments are consequence of the oxidative species produced in each case. In Photo-Fenton and UV/H_2O_2, the production of $OH^{\cdot}$ is higher than in Fenton, leading to a higher hydroxylation degree (see Eqs. (9) and (10)). On the other

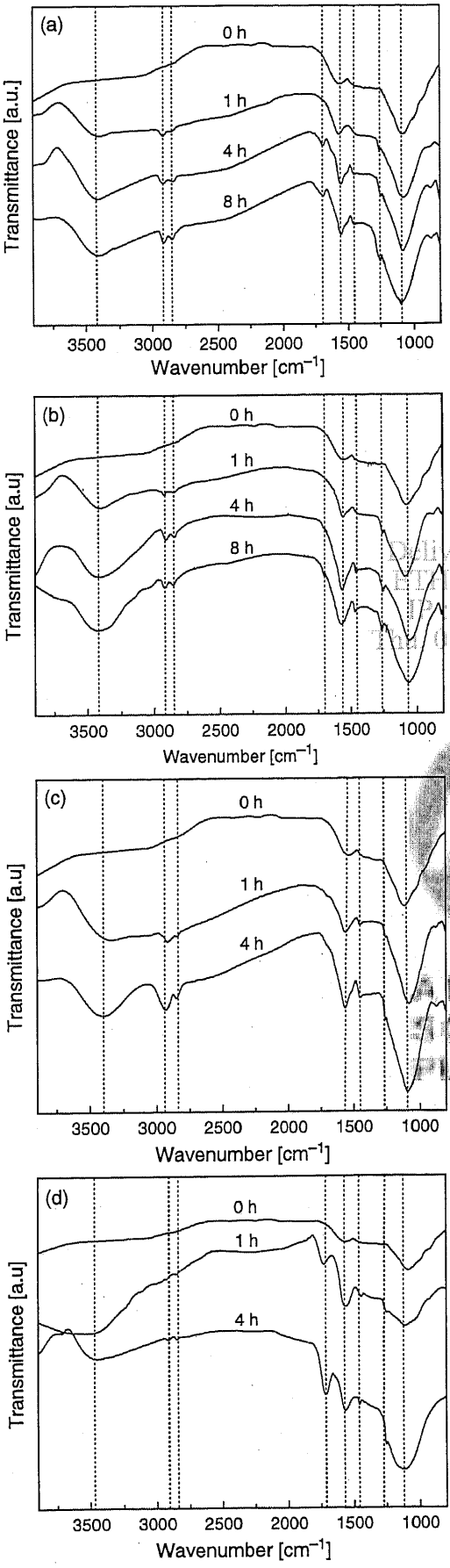

Fig. 2. FTIR spectra of MWCNT submitted to different treatments: (a) Fenton process, (b) Photofenton process, (c) UV/H_2O_2, (d) acid attack.

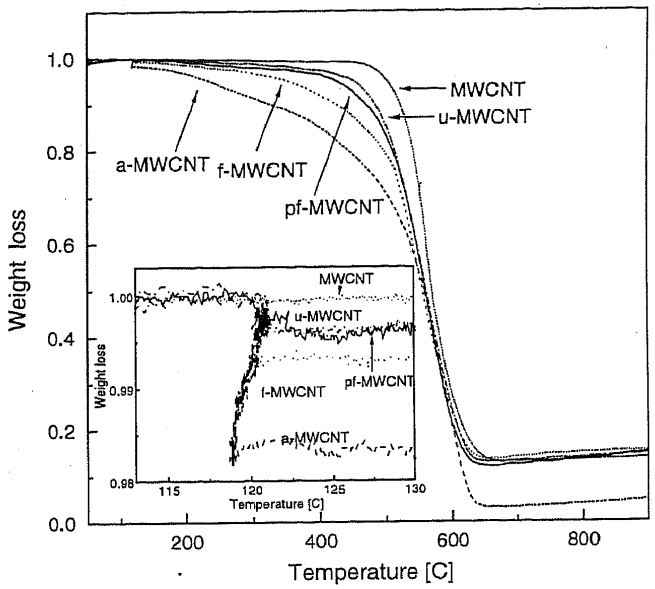

Fig. 3. TGA curves of MWCNT after different treatments during 4 h.

hand, the excess of OH$^{\cdot}$ and H_2O_2 in both processes may produce a diminution in the concentration of OH$^{\cdot}$ available for the oxidation of the CNT through the mechanism indicated in Eqs. (8) and (11), leading to lower carboxylation of CNT.

$$OH^{\cdot} + OH^{\cdot} \rightarrow H_2O + 1/2O_2 \qquad (11)$$

TGA thermograms of cleaned and treated MWCNT (Fig. 3) show that all oxidative treatments decrease the

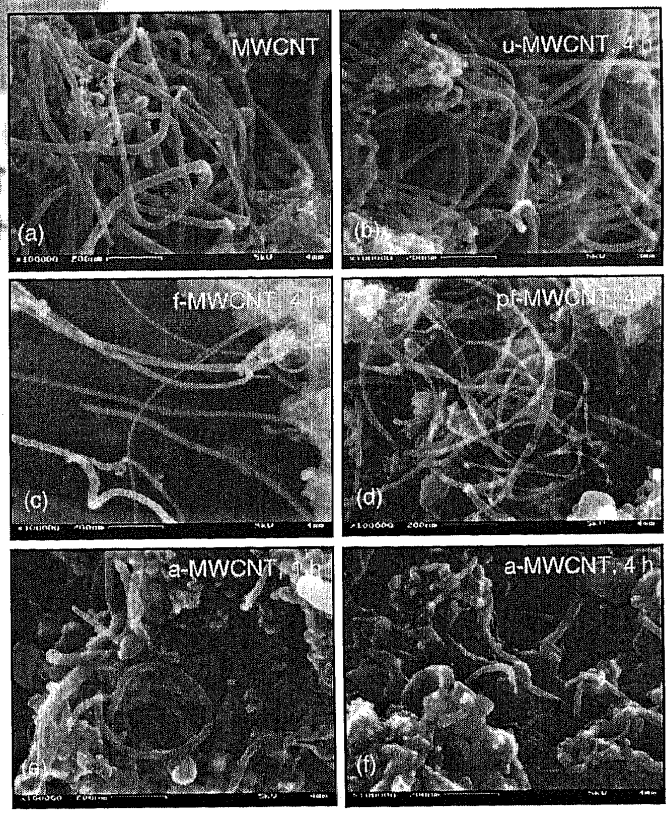

Fig. 4. FE-SEM micrograph of MWCNT after each treatment.

decomposition temperature as consequence of the partial oxidation of the carbon skeleton. Taking into account FTIR results, at higher degrees of carboxylation lower the decomposition temperature was. Clearly, the oxidative acid attack produces the most important reduction in the decomposition temperature indicating a higher damage on the CNT. In this figure it can be seen one step around 120 °C. This step was produced during the isothermal treatment of the sample at 120 °C during 20 min and it is associated with the amount of removable water. It can be noticed that the length of the step increases with the intensity of the FTIR peak of COOH (see Figs. 2(a–d)). This effect may be related with higher sorption of water by the hydrophilic COOH groups

On the other hand, it should be noticed that the remaining weight was lower in the case of oxidative acid attack during four hours due to the total elimination of the silica. It is in agreement with the disappearance of the peak at 1080 cm^{-1} in the FTIR spectrum associated to the four hours acid treatment.

Figure 4 shows FE-SEM micrographs of cleaned MWCNT before and after different oxidative treatments. The pristine nanotubes had a diameter between 20 and 40 nm and several micrometers length. As can be seen in Figures 4(b), (c) and (d), the nanotube morphology was not modified by the AOT treatments. On the other hand, Figures 4(e and f) show that the oxidative acid attack modified strongly the morphology of the MWCNT, a more aggregated system of short nanotubes is observed probably due to an excessive oxidation leading to the presence of a great quantity of functional groups everywhere on the nanotubes surfaces. By comparing Figures 4(e and f), it can be noted that the degradation of the MWCNT increased with the treatment time.

Figure 5 shows TEM images of MWCNT before and after treatment. These images support and complete the SEM observations. Pristine MWCNT are ca 20–40 nm wide, several μm long, with a channel of ca 10 nm wide. They are clearly multiple-wall CNT. Fenton treatment did not modify appreciably neither the morphology nor the length of the CNT. On the contrary, oxidative acid attack reduced notably their length and produced irregularities in the surface. These results agree with TGA analysis as the samples treated with $HNO_3 + H_2SO_4$ had a higher defect density and consequently the decomposition temperature was lower.

4. CONCLUSIONS

AOTs are useful for the controlled oxidation of CNT. The oxidation degree depends on the treatment time and the technology selected. Fenton process induces the formation of carboxylic groups on CNT, while Photo-Fenton and H_2O_2/UV generate mostly OH groups. The differences in behavior may be related with the amount of generated $OH^{\cdot}$ radicals and the nature of the secondary reactions. The morphology and structure of the CNT are not deeply damaged by AOT treatments. By comparison, the classical oxidant acid treatment with a mixture of HSO_4/HNO_3 acids produces a severe damage on the CNT, modifying both structure and morphology. Besides, the classical method introduces sulfates on the CNT surface, which are difficult to remove.

Acknowledgments: We thank the following institutions for their financial support: Universidad de Buenos Aires (UBACYT X-191); Consejo Nacional de Investigaciones Científicas y Técnicas - Argentina (PIP 5959 and PIP 5215); Agencia Nacional de Promoción Científica y Tecnológica - Argentina (PICT 10-25834 and PICT 33973); Gobierno Vasco/Eusko Jaurlaritza (IE05-146 and IT-365-07) and Ministerio de Educación y Ciencia/Feder (MAT2005-06530 and MAT2006-06331), Spain. Support from EC funded in 7th FP, NMP-213939 is thankfully appreciated.

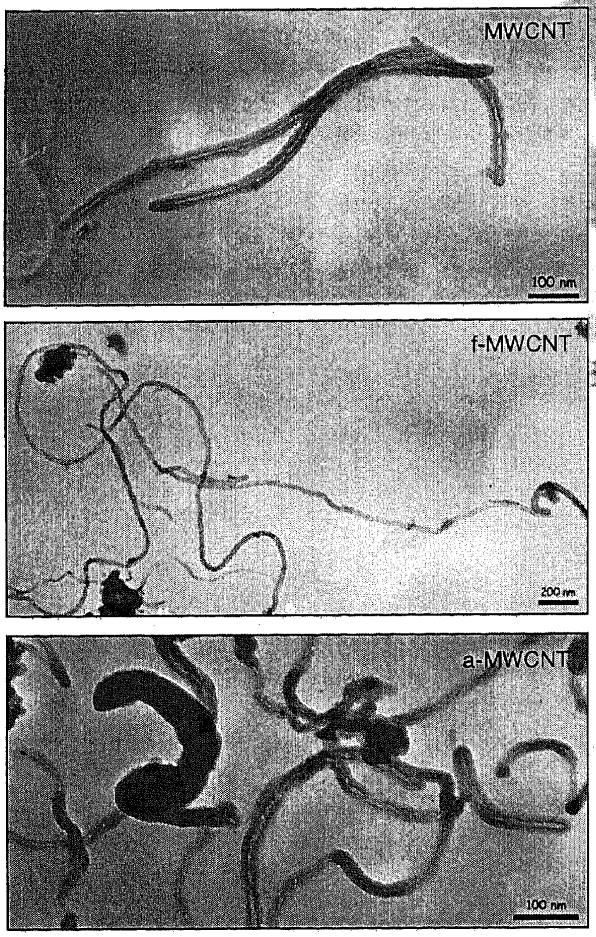

Fig. 5. TEM micrographs showing features of MWCNT before and after several treatments for 4 h.

References and Notes

1. J. L. Bahr, J. Yang, and D. V. Kosynkin, *J. Am. Ceram. Soc. J. Am. Chem. Soc.* 123, 6536 (2001).
2. X. W. Jiang, Y. Z. Bin, and M. Matsuo, *Polymer* 46, 7418 (2005).

3. S. Wang, R. Liang, B. Wang, and C. Zhang, *Chem. Phys. Lett.* 457, 371 (**2008**).
4. V. Datsyuk, M. Kalyva, K. Papagelis, J. Parthenios, D. Tasis. A. Siokou, I. Kallitsis, and G. Galiotis, *Carbon* 46, 833 (**2008**).
5. S. Goyanes, G. H. Rubiolo, A. Salazar, A. Jimeno, M. A. Corcuera, and I. Mondragon, *Diamond Relat. Mater.* 16, 412 (**2007**).
6. D. Bikiaris, A. Vassiliou, K. Chrissafis, K. M. Paraskevopoulos, A. Jannakoudakis and A. Docoslis, *Polym. Degrad. Stab.* 93, 952 (**2008**).
7. D. Y. Kim, C. M. Yang, H. Noguchi, M. Yamamoto, T. Ohba, H. Kanoh, and K. Kaneko, *Carbon* 46, 611 (**2008**).
8. M. L. Sham and J. K. Kim, *Carbon* 44, 768 (**2006**).
9. L. Zeng, W. Wang, J. Liang, Z. Wang, Y. Xia, D. L. X. Ren, N. Yao, and B. Zhang, *Mater. Chem. Phys.* 108, 82 (**2008**).
10. Y. Ying, R. K. Saini, F. Liang, A. K. Sadana, and W. E. Billups, *Org. Lett.* 5, 1471 (**2003**).
11. W. Li, Y. Bai, Y. Zhang, M. Sun, R. Cheng, X. Xu, Y. Chen, and Y. Mo, *Synth. Met.* 155, 509 (**2005**).
12. J. J. Pignatello, *Environ. Sci. Technol.* 26, 944 (**1992**).
13. J. J. Pignatello, D. Liu, and P. Huston, *Environ. Sci. Technol.* 33, 1832 (**1999**).
14. J. De Laat, H. Gallard, S. Ancelin, and B. Legube, *Chemosphere* 39, 2693 (**1999**).
15. A. M. Rao, *J. Mater. Res.* 8, 2277 (**1993**).
16. M. Escobar, M. S. Moreno, R. J. Candal, M. C. Marchi, A. Caso, P. I. Polosecki, G. H. Rubiolo, and S. Goyanes, *Appl. Surf. Sci.* 254, 251 (**2007**).

Received: 30 May 2008. Accepted: 31 December 2008.